Available online at www.sciencedirect.com
ScienceDirect
Bioelectrochemistry 70 (2007) 235–244
Bioelectrochemistry
www.elsevier.com/locate/bioelechem

DNA/Poly(*p*-aminobenzensulfonic acid) composite bi-layer modified glassy carbon electrode for determination of dopamine and uric acid under coexistence of ascorbic acid

Xiangqin Lin *, Guangfeng Kang, Liping Lu

Department of Chemistry, University of Science and Technology of China, Hefei 230026, PR China

Received 20 June 2005; received in revised form 18 February 2006; accepted 20 February 2006
Available online 30 August 2006

Abstract

A nano-composite of DNA/poly(*p*-aminobenzensulfonic acid) bi-layer modified glassy carbon electrode as a biosensor was fabricated by electro-deposition method. The DNA layer was electrochemically deposited on the top of electropolymerized layer of poly(*p*-aminobenzensulfonic acid) (Pp-ABSA). Scanning electron microscopy, X-ray photoelectron spectroscopy and electrochemical impedance spectrum were used for characterization. It demonstrated that the deposited Pp-ABSA formed a 2-D fractal patterned nano-structure on the electrode surface, and which was further covered by a uniform thin DNA layer. Cyclic voltammetry and electrochemical impedance spectrum were used to characterize the deposition, and demonstrated the conductivity of the Pp-ABSA layer. The biosensor was applied to the detection of dopamine (DA) and uric acid (UA) in the presence of ascorbic acid (AA). In comparison with DNA and Pp-ABSA single layer modified electrodes, the composite bi-layer modification provided superior electrocatalytic actively towards the oxidation of DA, UA and AA, and separated the originally overlapped differential pulse voltammetric signals of UA, DA and AA oxidation at the bare electrode into three well-defined peaks at pH 7 solution. The peak separation between AA and DA, AA and UA was 176 mV and 312 mV, respectively. In the presence of 1.0 mM AA, the anodic peak current was a linear function of the concentration of DA in the range 0.19–13 μM. The detection limit was 88 nM DA ($s/n=3$). The anodic peak current of UA was also a linear function of concentration in the range 0.4–23 μM with a detection limit of 0.19 μM in the presence of 0.5 mM AA. The superior sensing ability was attributed to the composite nano-structure. An interaction mechanism was proposed.

Keywords: DNA; Poly(*p*-aminobenzensulfonic acid); Dopamine; Uric acid; Nanostructure

1. Introduction

Deoxyribonucleic acid (DNA) as an important biological macromolecule has been paid much attention in the recent years. It is not only due to the intriguing genetic information of the molecule but also the possible utilities of its efficient electro-conductivity of the long chain [1–7], which has been considered as the function of the rich p-electron of base-stacking along its double helical backbone. On the other hand, interaction of DNA with many kinds of bioactive species has been found, which provided a base for molecular recognition not only for DNA hybridization but also for sensing of bioactive species [8,9]. The interaction of catecholamines with DNA has also been observed and provided a novel way for fabrication of neurotransmitter biosensors [10]. Electrochemical sensors based on DNA recognition have been reported for dopamine (DA), norepinephrine, uric acid (UA) determination in the presence of ascorbic acid (AA) [11,12]. Electrochemical deposition of DNA on electrode surfaces has been considered for obtaining a conductive thin layer of nano-structures and enhancing the electrode surface area for construction of efficient biosensors [13–15].

To prevent denature of DNA grafted on electrode surfaces, nano-composite of DNA could be considered. A DNA/nano-Au composite has been found for fabrication of biosensors [12]. It is believed that conducting polymers may offer an efficient way for DNA grafting [9]. The conducting polymers may be able to

* Corresponding author. Tel.: +86 551 3606646; fax: +86 551 3601592.
E-mail address: xqlin@ustc.edu.cn (X. Lin).

1567-5394/$ - see front matter © 2006 Elsevier B.V. All rights reserved.
doi:10.1016/j.bioelechem.2006.02.003

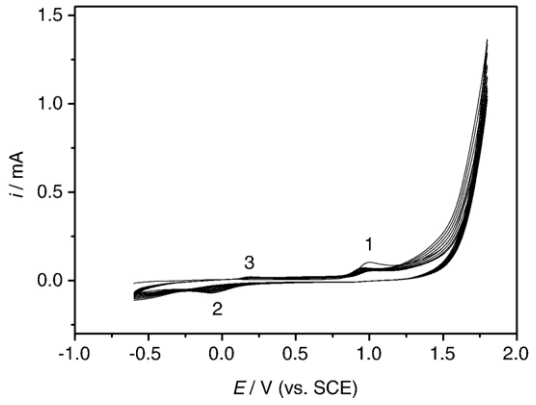

Fig. 1. Multicycle CV for Pp-ABSA deposition at GCE. Solution: 2.0 mM p-ABSA+0.1 M pH 7.0 PBS+0.5 M KCl; Scan rate: 100 mV/s.

modulate long-range charge transport through strong interactions with attached DNA molecules [16]. The immobilization of DNA on conducting polymers has been accomplished mainly by two approaches involving incorporation of nucleotides into the polymer matrix during the growth of the conducting polymer [17–21] and fabrication by immobilizing DNA molecules on the top of the polymer layer [22–24]. The later structure can be formed by either direct absorption or covalent attachment (directly or through a bridging medium) of DNA on the polymer layer. However, to our best of knowledge, this stratagem of layer-by-layer modification of DNA and conducting polymers has never been reported for fabrication of electrochemical sensors of DA and UA.

DA and UA are commonly existed in body fluids and extreme abnormalities of their concentration levels may lead to several diseases such as Parkinson's, Alzheimer and gout [25,26]. Therefore, the detection of their concentration is important not only for clinical diagnostics but also for pathological research. A major obstacle in monitoring DA and UA using electrochemical technique is the influence from the co-existence of large amount of AA, since AA can also be oxidized with large overpotentials in the result of current overlapping at bare electrodes. Recently, various chemical modification of electrode surface has been used to overcome this problem by either reducing the overpotential of AA oxidation or preventing the approach of AA anions to the electrode surface [27–40].

In the recent years, we have investigated the electro-deposition of Pp-ABSA and catalytic activities of the Pp-ABSA modified electrode. This report describes the use of electro-deposited Pp-ABSA as a matrix for DNA immobilization in order to fabricate biosensors for the determination of DA and UA simultaneously in the presence of large amount of AA. A novel biosensor was obtained, and this sensor not only exhibited strong catalytic activity toward the oxidation of DA, UA and AA but also separated their voltammetric responses into three well-defined peaks with large potential separations in neutral solutions. The sensor was sensitive with detection limit of 88 nM DA and 0.19 μM UA in the presence of large amount of AA.

2. Experiment

2.1. Chemicals and materials

Calf thymus DNA (ct-DNA, 23000 bp, $OD_{260}/OD_{280}>1.8$) was obtained from Sino-American Biotechnology Co. Dopamine (DA) was purchased from Sigma. *P*-aminobenzenesulfonic acid (P-ABSA), uric acid (UA) and ascorbic acid (AA) were from Chemical Reagent Company of Shanghai. These compounds were used as received without further purification. All other chemicals were of analytical grade. High purity N_2 and doubly distilled water were used.

The 0.1 M phosphate buffer solution (PBS) containing 0.5 M KCl was used as the supporting electrolyte solution. To mimic biological environments, pH 7.0 was selected unless stated otherwise. The 0.1 M pH 7.0 PBS+0.5 M KCl solution is denoted as the solution A.

2.2. Apparatus

Cyclic voltammetry (CV) and differential pulse voltammetry (DPV) were recorded on a CHI 832 electrochemical analyzer (Cheng-Hua, Shanghai, China). Electrochemical impedance spectroscopy (EIS) was conducted on a CHI 660A workstation (Cheng-Hua, Shanghai, China). All electrochemical experiments were carried out using a three-electrode system consisted of a working electrode, a platinum wire auxiliary electrode and a saturated calomel reference electrode (SCE). A glassy carbon disk electrode (GCE, 4 mm in diameter) was used as the basal electrode for surface modification and construction of the biosensor. Electrochemical solutions were thoroughly deoxygenated by N_2 bubbling before use and maintained N_2 atmosphere through out the experiment. All experiments were carried out at room temperature.

Scanning electron microscopy (SEM) images were obtained at a JSM-6700F (JEOL) Field Emission Scanning Electron microanalyser.

X-ray photoelectron spectroscopy (XPS) measurement was performed on an ESCALAB MK2 spectrometer (VG, UK) with Mg K-Alpha X-ray radiation source.

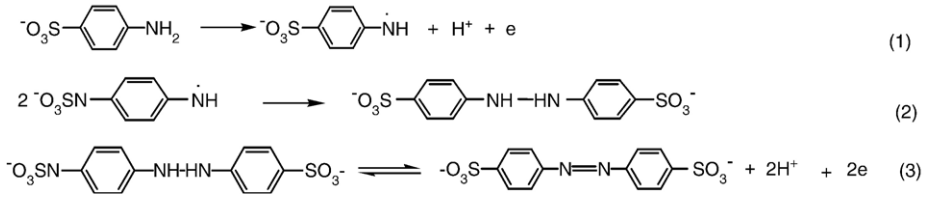

Scheme 1.

2.3. Preparation of electrodes

Prior to use, the GCE was successively polished with 1.0, 0.3, 0.05 μm alumina slurry, ultrasonic cleaning in ethanol, water for 5 min each time.

The GCE was dipped into the p-ABSA solution for electrochemical polymerization and deposition of Pp-ABSA. The obtained electrode is denoted as Pp-ABSA/GCE in this report. CV potential cycling was found to have advantages for the modification, and the CV parameters including the scan rate (v), the potential range for the cycling, the cycle numbers, the composition of the deposition solution were optimized as 100 mV/s, in between −0.6 and +1.8 V (vs. SCE), 10 cycles, 2.0 mM p-ABSA/solution A, respectively.

The prepared Pp-ABSA/GCE was cleaned with water, dipped in a ct-DNA solution for DNA electro-deposition. The deposition was carried out under constant potential of +1.5 V for a certain time in 0.1 mg/ml ct-DNA/solution A [12]. It was found that 30 min deposition is proper for obtaining a high quality sensing electrode, denoted as DNA/Pp-ABS/GCE. For comparison, the same deposition was made on a bare GCE to prepare a DNA modified GCE without the Pp-ABSA interlayer, denoted as DNA/GCE.

All these electrodes were stored in water after use.

3. Results and discussion

3.1. Characterization of modified electrodes

3.1.1. Electropolymerization and deposition of p-ABSA

The progress of CV deposition of Pp-ABSA on a GCE is shown in Fig. 1. The multicycle CV curve in 2.0 mM p-ABSA solution showed 3 major voltammetric peaks at about 0.94 V (peak 1), −0.05 V (peak 2) and 0.21 V (peak 3). Peak 1 is attributed to the one-electron oxidation of amino group at p-ABSA. Peak 2 and 3 can be attributed to the redox reaction of the deposited Pp-ABSA.

The deposition mechanism can be expressed in Scheme 1. The p-ABSA was first oxidized to its free radicals at 0.94 V, which combined together rapidly, forming the head-to-head dimmer, Pp-ABSA. And the Pp-ABSA have a redox step at a middle potential (E_m) of about 0.12 V.

Similar mechanism was also proposed [41]. The p-ABSA could not fully polymerize to form a head to tail long chain because of the existence of the sulfonic group at the opposite position, which plays steric hindrance effect and strong electron-withdrawing effect for the polymerization [42–44].

3.1.2. Morphology of the modified surfaces

Fig. 2 shows the SEM images of the Pp-ABSA/GCE and DNA/Pp-ABSA/GCE. It can be seen that the Pp-ABSA deposited on the GCE surface was assembled to form a pattern of grass like branches (Fig. 2a). This fractal pattern was consisted of particles of 50–300 nm in diameter separately distributed on the electrode surface, which can be seen from the enlarged image shown in Fig. 2b. The fractal pattern should be assembled by the surface diffusion of nano-clusters on the substrate [45], and the patterned distribution of the Pp-ABSA nano-clusters provided large active surface is advantageous to electrochemical sensing. After the DNA deposition, this fractal structure was completely covered by the DNA deposited layer, as shown in Fig. 2c.

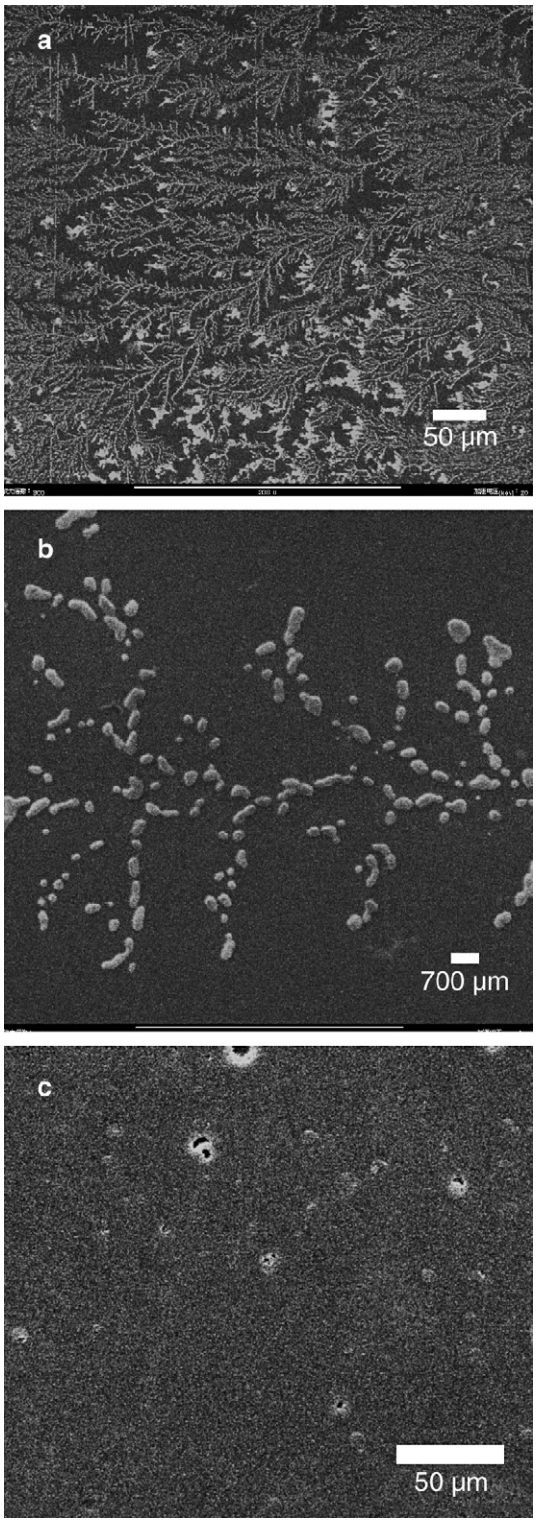

Fig. 2. SEM images of the Pp-ABSA/GCE (a, b), DNA/Pp-ABSA/GCE (c).

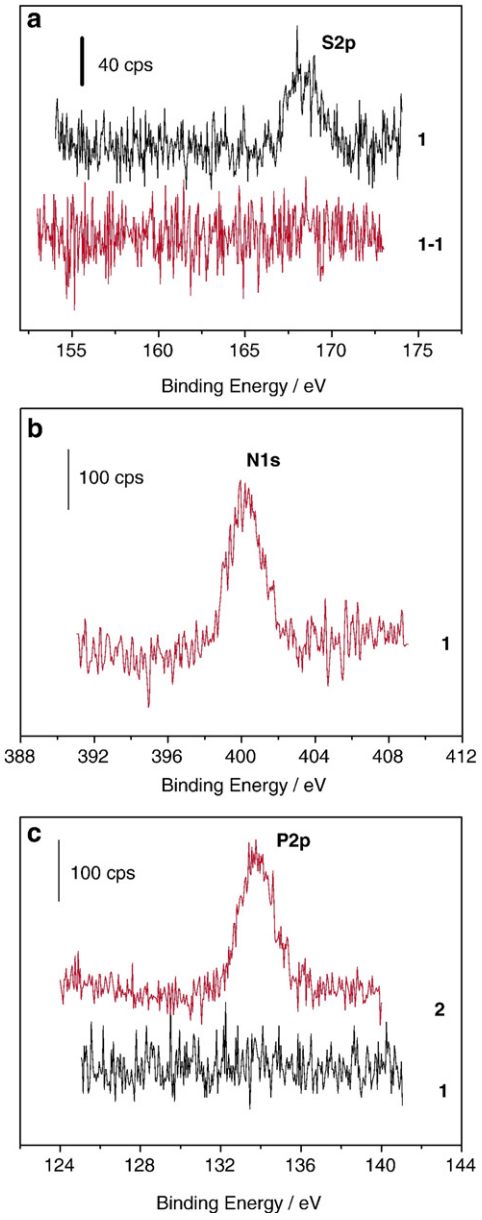

Fig. 3. XPS spectra of S2p (a), N1s (b) and P2p region (c) for Pp-ABSA/GCE (1), DNA/Pp-ABSA/GCE (2), and the Pp-ABSA/GCE after being ultrasonicated (1–1).

The fractal deposition of Pp-ABSA on the GCE surface created a two-dimensional nano-structure for the further fabrication of DNA layer. It can be noted that the fractal patterns covered only about 20% of the electrode surface, and further deposited DNA molecules, which may form nano-netting structures on the surface [13–15], should stick on both the Pp-ABSA clusters and the remaining bare GCE surface, in result of a composite of three dimensional structures. Since the Pp-ABSA dimmer has large conjugation, the aggregated Pp-ABSA cluster can be expected to have electric conductivity, the fractal distribution of the Pp-ABSA nano-clusters provided a nano-electrode array. Thus, the second layer deposition, the DNA deposition, was conducted on the nano-electrode array of the polymer. In comparison with normally deposited nano-particles, the fractal deposition can provide much more "dilute" deposition. As seen from Fig. 2b, the nano-particles in the fractal pattern were well separated each other with average distance much larger than the average size, the advantages of nano-electrode array could thus be performed. The fractal deposition of nano-particles is obviously a useful stratagem for fabrication of high efficiency electrochemical sensors.

3.1.3. XPS spectra

XPS was used to examine the elemental distribution on the electrode surfaces. The result is shown in Fig. 3. As shown in Fig. 3a curve 1, the S_{2p} peak appeared at 168 eV is consistent with the existence of $-SO_3^-$ groups in the deposited Pp-ABSA at the Pp-ABSA/GCE. Since some amine containing compounds could firmly link on the surface of carbon electrodes by the formation of C–N bound during electrochemical oxidation [46,47], XPS spectrum was taken after this electrode being ultrasonicated in ethanol and H_2O successively for 10 min each time. The result is shown in Fig. 3a curve 1–1, no S_{2p} peak remained there. The disappearance of 167 eV peak after ultrasonication indicated that the p-ABSA did not attach to the GCE surface by covalent linkages, but dimerized and attached to the electrode surface by adsorption.

The XPS of Pp-ABSA/GCE showed also a characteristic N1s band at 400.45 eV (Fig. 3b), which is consistent with the formation of −N=N-bond in the dimer.

The spectrum of the DNA/p-ABSA/GCE was different from that of the p-ABSA/GCE, as shown in Fig. 3c. The existence of P_{2p} band at 133.7 eV demonstrated the deposition of DNA on the electrode.

3.1.4. Electrochemical characterization of modified electrodes

The prepared DNA/Pp-ABSA/GCE, Pp-ABSA/GCE, DNA/GCE were characterized by CV of $Ru(NH_3)_6^{3+}$ cations and $Fe(CN)_6^{3-}$ anions in comparison with a bare GCE. The $Ru(NH_3)_6^{3+}$ gave a redox peaks at about −0.18 V vs. SCE at these electrodes. However, the cathodic peak current of $Ru(NH_3)_6^{3+}$ at three modified electrode was higher than at bare GCE, indicating a negatively charged modified layer that could attract the positively charged species.

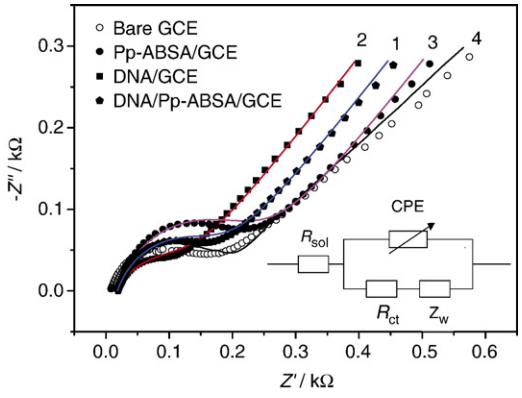

Fig. 4. EIS spectra of the DNA/Pp-ABSA/GCE (1), the Pp-ABSA/GCE (2), the DNA/GCE (3) and a bare GCE (4) in 10 mM $Fe(CN)_6^{3-}$ + 10 mM $Fe(CN)_6^{4-}$. Inset: the equivalent circuit.

Table 1
EIS data of GCE, Pp-ABSA/GCE, DNA/GCE and DNA/Pp-ABSA/GCE in 10 mM $Fe(CN)_6^{3-/4-}$

Electrode	R_{sol}/Ω	Φ	$B/(S\ cm^{-2}\ s^{-n})$	$s/(\Omega\ cm^2\ s^{-1/2})$	R_{ct}/Ω
GCE	8.22	0.776	3.00e− 5	188	180
Pp-ABSA/GCE	16.2	0.620	5.00e− 4	143	132
DNA/GCE	16.4	0.757	2.00e− 4	136	225
DNA/Pp-ABSA/GCE	18.2	0.737	2.00e− 4	136	169

The redox reaction of $Fe(CN)_6^{3-}$ appeared at a middle potential (E_m) of 0.270 V at GCE, however, which is shifted to 0.290 V at the three modified electrodes, indicating an interaction between the $Fe(CN)_6^{3-/4-}$ and the DNA and Pp-ABSA layers. In addition, both the cathodic and anodic peak currents increased to about two times at three modified electrode, indicating the effective surface area of these electrode was enlarged by two-fold due to the conductive Pp-ABAS and DNA modified layers.

The modified electrodes were further evaluated by EIS in 10 mM $Fe(CN)_6^{3-/4-}$ solution in comparison with a bare GCE. The EIS spectra were obtained shown in Fig. 4, which were fitted by digital simulation based on the equivalent circuit (inset). Considering the complexity of the modified structure, a constant phase angle element (CPE) was used for construction of the equivalent circuit. The total impedence of the equivalent circuit, Z_{total}, can be expressed as $Z_{total}=R_{sol}+1/(1/Z_{CPE}+1/(R_{ct}+Z_w))$, where $Z_{CPE}=[B(j\omega)^{\Phi}]^{-1}$, $j=(-1)^{1/2}$, ω is the angular frequency, B and Φ ($0<\Phi=1$) are frequency dependent constants [19], and $Z_w=s(1-j)/\omega^{1/2}$, where s is a constant related to Warburg impedance. Thus, R_{sol}, Φ, B, s and R_{ct} five parameters can be obtained from the fitting, which are summarized in Table 1.

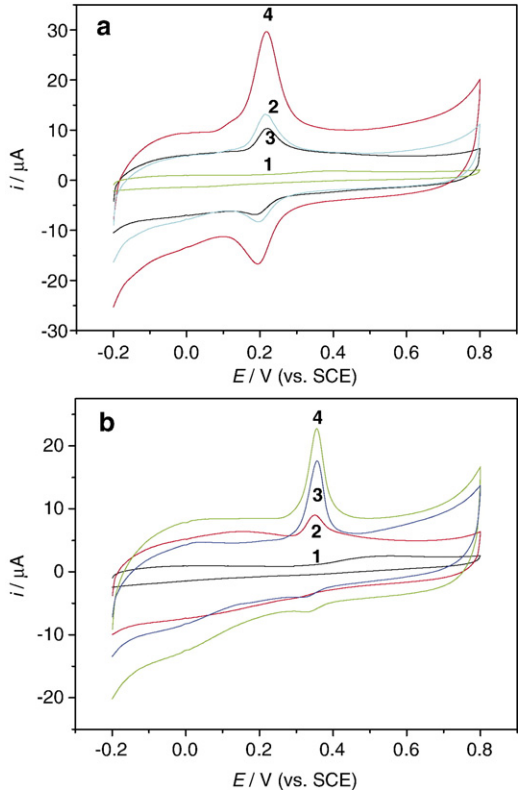

Fig. 5. CVs of 50 mM DA (a) and 50 mM UA (b) at bare GCE (1), Pp-ABSA/GCE (2), DNA/GCE (3) and DNA/Pp-ABSA/GCE (4) in pH 7.0 PBS. Scan rate: 50 mV/s.

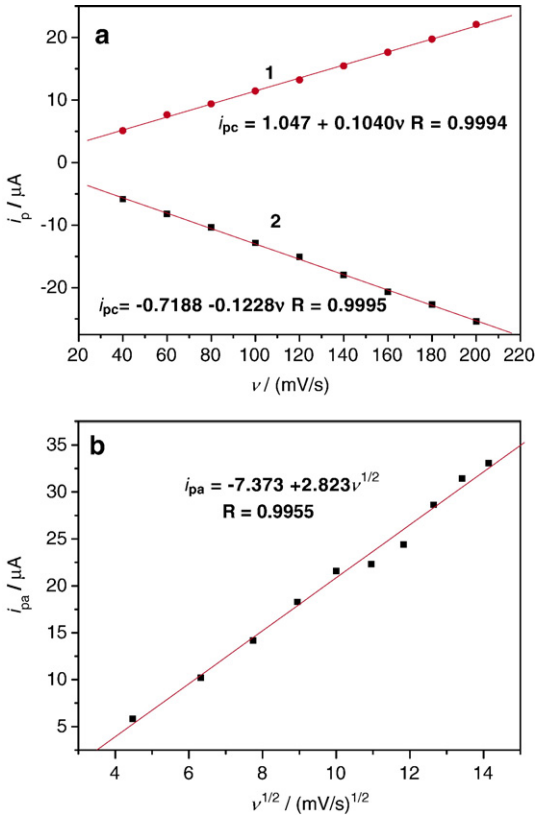

Fig. 6. Plot of anodic (1) and cathodic (2) peak current of 50 mM DA (a) and 50 mM UA (b) versus the scan rate at DNA/Pp-ABSA/GCE.

It can be seen from Table 1 that the R_{sol} of all electrodes are less than 20 Ω, thus minimal potential error would be generated for currents in μA scale. The R_{ct}, the electron transfer resistance, is characteristic for evaluation of the electron transfer rate constant. The R_{ct} value was reduced to about 2/3 by the surface modification of Pp-ABSA layer on GCE. The R_{ct} value was reduced to about 3/4 at the DNA/Pp-ABSA/GCE in comparison with that at the DNA/GCE. Thus demonstrated the conductivity of the surface modified Pp-ABSA nano-particles.

3.2. Electrochemical behavior of DA, UA and AA

3.2.1. CVs of DA and UA

The preliminary study showed that the DNA/Pp-ABSA/GCE had a significant electrocatalytic activity toward the oxidation reactions of DA and UA. The CV curves of these compounds at different electrodes are presented in Fig. 5.

As shown in Fig. 5a, DA presented a drawn out CV peaks with a small anodic peak at about 0.40 V and a small re-reduction peak at about 0.05 V at GCE (curve 1). However, a couple of well behaved CV peaks at 0.210 and 0.195 V appeared at the Pp-ABSA/GCE. About 4-fold anodic peak current was obtained in comparison with that at GCE (curve 2).

The 190 mV negative potential shift indicates the catalytic activity of the electrode, and the current increase can be attributed mainly to a surface accumulation ability of the two-dimensional dimer clusters modified layer. The DNA/GCE also catalyzed the oxidation of DA, giving the oxidation peak at 0.210 V, however, with only 3-fold peak current (curve 3). This is not surprising since DA can be accumulated on DNA before electrochemical oxidation [12]. However, the DNA/Pp-ABSA/GCE gave the oxidation peak at also 0.21 V but with about 20-fold peak current (curve 4). This peak current is about 3 times larger than the addition of the peak current at the DNA/GCE and the peak current at the Pp-ABSA/GCE, indicating the existence of some kinds of interactions between the Pp-ABSA layer and the DNA layer for the DA oxidation. The extra current enhancement is possibly due to an enhancement of the efficiency of electron transfer for the DNA confined DA molecules, since the electronic conductive Pp-ABSA clusters may provided better electric connections between the DNA chains and the GCE surface. Certainly, the re-reduction peak at 0.20 V appeared at the Pp-ABSA/GCE, which is only 10 mV apart from the anodic peak, showing typical phenomena for a surface conformed redox reaction.

Fig. 5b shows the CV for UA oxidation. As seen from curve 1, UA gives a broad oxidation peak at about 0.5 V at GCE. However, a sharp peak appeared at 0.35, 0.36 and 0.36 V at Pp-ABSA/GCE, DNA/GCE and DNA/Pp-ABSA/GCE, respectively (curve 2–4), showing all the three electrodes had strong electrocatalytic activity toward the UA oxidation. And, 3-fold

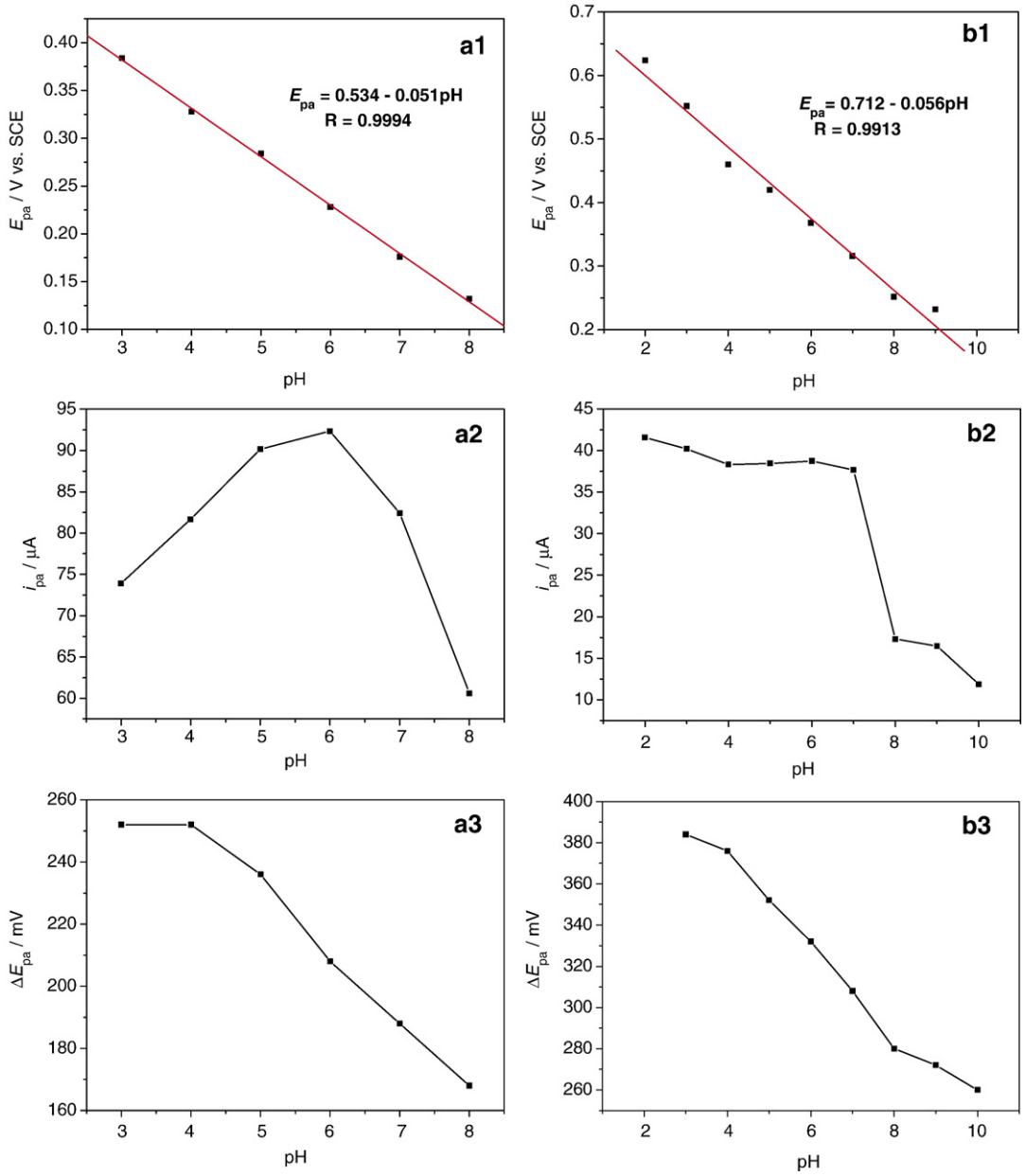

Fig. 7. The effect of pH on E_{pa} (1), i_{pa} (2) and ΔE_{pa} (E_{pa} vs. the AA anodic peak potential) (3) for DA (a) and UA (b) at DNA/Pp-ABSA/GCE. DPV: Scan rate: 20 mVs^{-1}, Amplitude: 50 mV, Pulse width: 50 ms, Pulse period: 200 ms.

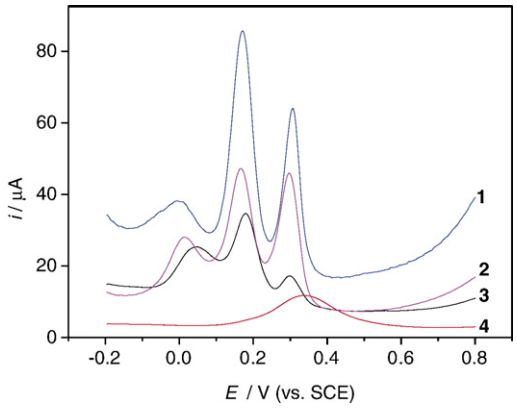

Fig. 8. DPV curves in 0.1 M PBS containing 50≥M DA, 50≥M UA and 1.0 mM AA at the DNA/Pp-ABSA/GCE (1), the DNA/GCE (2), the Pp-ABSA/GCE (3), and a bare GCE (4). DPV: Scan rate: 20 mV/s; Amplitude: 50 mV; Pulse width: 50 ms; Pulse period: 200 ms.

peak current at the Pp-ABSA/GCE, and about 10-fold increase at both the DNA/GCE and the DNA/Pp-ABSA/GCE were observed in comparison with that at GCE. The current sensitivity was almost the same for the later two electrodes, the existence of the Pp-ABSA clusters seemed to not play a significant role in the UA oxidation, indicating a different interaction mode for UA and DNA.

3.2.2. The effect of scan rate

The effect of scan rate on the peak current of DA and UA at the DNA/Pp-ABSA/GCE were investigated. The results are shown in Fig. 6. As shown in Fig. 6a, the peak current (i_{pa}, i_{pc}) of DA was linearly proportional to the scan rate up to 200 mV/s, $i_{pa}=1.05+0.104v$ (μA, mV/s, $R=0.9994$), which is expected for the redox reaction of surface adsorbed species. The i_{pa}/i_{pc} ratio remained almost equal to unity if the switching potential is not far from the peak. However, as shown in Fig. 6b, the i_{pa} of UA at DNA/Pp-ABSA/GCE was proportional to the square root of scan rate over the range of 20–200 mV/s, $i_{pa}=-7.373+2.823v^{1/2}$ (μA, mV/s, $R=0.9955$), suggesting a diffusion controlled process.

3.2.3. The effect of pH

For DA and UA determination, the pH effect on DPV signals at the DNA/Pp-ABSA/GCE was examined, as shown in Fig. 7. The peak potential of DA oxidation shifted negatively at a slope of −51 mV per pH unit in the range of 3–8 (Fig. 7a1), indicating equal number of electrons and protons involved in the oxidation process. The peak current was plotted versus pH in Fig. 7a2, a maximum at about pH 6 was found. Since AA also showed a DPV peak, the peak separation of DA and AA (denoted as ΔE_{pa}) was used as the criteria to evaluate the selectivity of the catalytic system. The result showed that the ΔE_{pa} decreased with the increase of pH value from 3 to 8 (Fig. 7a3).

The DPV peak potential of UA oxidation shifted also negatively at a slope of −56 mV per pH unit in the range of 2–9 (Fig. 7b1), which is in agreement with the $2e/2H^+$ reaction. The peak current of UA was almost constant in the pH range of 2–7 and decreased sharply from pH 7 to 8 (Fig. 7b2), which was

Table 2
The DVP data at three modified electrodes for the oxidation of AA, DA and UA in a mixture of 50 μM DA+50 μM UA+1.0 mM AA

Electrode	E_{pa}/mV vs. SCE			ΔE_{pa}/mV		i_{pa}/μA		
	AA	DA	UA	DA	UA	AA	DA	UA
Pp-ABSA/GCE	36.0	180	300	144	264	6.65	17.0	5.32
DNA/GCE	16.0	168	296	152	280	10.2	26.2	30.7
DNA/Pp-ABSA/GCE	−4.00	172	308	176	312	8.42	57.7	41.4

little higher than the pK value of free UA species. The ΔE_{pa} of UA versus pH plot is shown in Fig. 7b3. It also shows a decrease with the increase of pH in the whole range from 2 to 9.

In the view of determination of both DA and UA in the presence of AA, it is obvious that the pH value lower than neutral is favorable for having higher sensitivity and higher selectivity. However, in order to mimic the physiological environment, pH 7.0 was still chosen for study.

3.2.4. DPV signal of the mixture of DA, UA and AA

DPV technique can provide a better peak resolution and current sensitivity, which is very suitable for simultaneous determination of species in mixture. Fig. 8 shows the DPV curves in 50 mM UA+50 mM DA+1.0 mM AA mixture solution at the DNA/Pp-ABSA/GCE in comparison with that at the Pp-ABSA/GCE, the DNA/GCE, and a bare GCE.

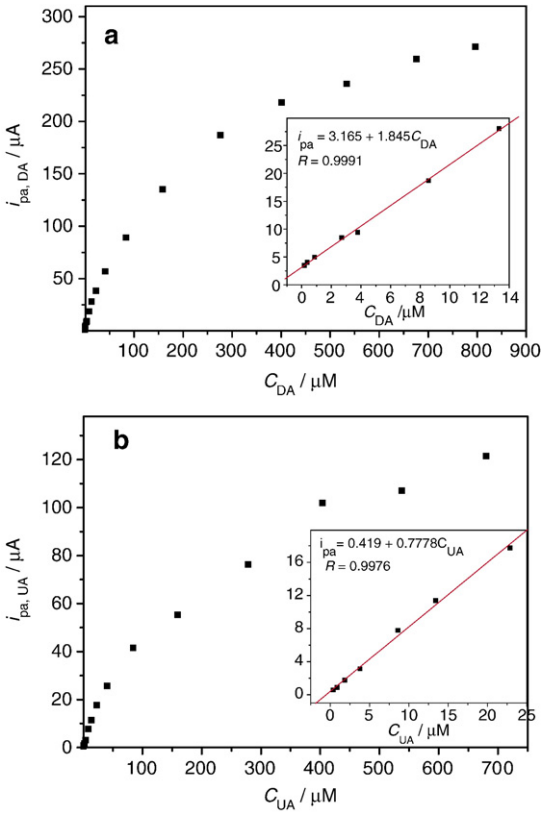

Fig. 9. Plot of DPV peak current at the DNA/Pp-ABSA/GCE as a function of DA (a) and UA (b) concentration in 0.1 M pH 7.0 PBS+1.0 mM AA. Insets: The linear plots of peak current vs. concentration (DA concentration range: 0.19–13 μM, $R=0.9991$; UA: 0.38–23 μM, $R=0.9976$).

It can be seen clearly that that the oxidation peaks of AA, DA and UA at the DNA/Pp-ABSA/GCE appeared at −0.004, 0.308 and 0.172 V, respectively, which are well separated each other with relatively flat baselines (curve 1). These peaks appeared at 0.036, 0.180 and 0.300 V at the Pp-ABSA/GCE (curve 2), and 0.016, 0.168 and 0.296 V at the DNA/GCE (curve 3) respectively. Comparatively, only one broad, small anodic peak at about 0.336 V appeared at a bare GCE (curve 4). The ΔE_{pa} value can be estimated as 176 mV for DA and 312 mV for UA. The results have been summarized in Table 2. It can be seen from the table, all the three modified electrodes gave three separated DPV peaks for these three species, however, Pp-ABSA/GCE obviously is the best one for high potential resolution, high sensitivity and suitable for the use of simultaneous determination.

From the above comparison of the voltammetric behaviours of these modified electrodes, we may believe that the electro-catalytic activity of the DNA/Pp-ABSA/GCE come from the cooperative effect of the two modified layers, the DNA and Pp-ABSA. The interaction between these layers can be ascribed. Comparing with other polyamines, the Pp-ABSA dimer molecules have more freedom in the surface assembling and stronger inter-molecular interaction, for which the well organized 2-D fractal can be formed. Thus, strong inter-layer interactions can be built for the layer being covered by the DNA.

On the other hand, DNA has also a strong ability to interact with various molecules [10,48–50]. We may suppose that the Pp-ABSA and DNA formed a supermolecule through the strong interaction between them, and in which the inner core of double helical DNA may be composed of a stacked array of heterocyclic base pairs and aromatic rings. The stacking of conjugated aromatic rings from the dimer molecules with the base pairs in DNA molecules might provide a perfect pathway for charge transport (CT) from the conducting DNA chains to more remote distance, to the GCE and facilitate the electron transfer processes.

3.3. Determination of DA and UA in the presence of AA

The DNA/Pp-ABSA/GCE was used for simultaneous determination of DA and UA in the presence of large amount of AA by using DPV technique. The result is shown in Fig. 9.

The dependence of the peak current on the concentration of DA in the presence of 1.0 mM AA is presented in Fig. 9a. A linear relationship was obtained over the concentration range from 0.19 to 13 μM with a detection limit of 88 nM ($s/n=3$) (the inset). The linear regression equation was: i (μA) = 3.165 + 1.845 C_{DA} (μM) with a correlation coefficient (R) of 0.9991. Thus, it may be concluded that more than 10^3 fold AA did not interfere the detection of DA. The excellent selectivity would be partly attributed to the high electron density and fruitful negative charge of the modified layers, which could strongly attract DA cations while repelling AA anions in the neutral environment.

Fig. 9b shows the peak current of UA versus the concentration in the presence of 0.5 mM AA. The result showed that peak current was linearly proportional to the UA concentration in the range of 0.38–23 μM a detection limit of 0.19 μM (the inset). The linear regression equation was: i (μA) = 0.418 + 0.7778 C_{UA} (μM) ($R=0.998$). Thus, it may be concluded that more than 500 fold AA did not interfere the detection of UA.

It is also noted that both the peak current response of DA and UA was not linear in wider ranges of concentration, as shown in Fig. 9a and b. This is easy to understand because the DA oxidation was an absorption-controlled process, and the adsorption accumulation could be saturated. The oxidation of UA was a diffusion-controlled process, the non-linear relation may indicate that the UA should also interact with the DNA layer and be accumulated on the electrode surface before the oxidation. This is in agreement with the data shown in Fig. 8 and Table 2, where the UA current was much higher at DNA modified electrodes than at Pp-ABSA/GCE, although both the accumulation process was fast and no significant time effect was observed.

3.4. Interferences

The major interference was from AA, which is discussed in the above. Other influences from common co-existing substances were also investigated. It was found that no interference for the detection of UA or DA was observed for these compounds (tolerance ratio): Citric acid (1000), glucose (400), tyrosine (400) and tryptophan (400).

4. Conclusion

The DNA/Pp-ABSA/GCE was fabricated by electrochemical deposition of DNA on the Pp-ABSA fractal modified GCE electrode for simultaneous determination of DA and UA in the presence of large amount of AA. This electrochemical sensor exhibited both strong electro-catalytic activity toward DA, UA and AA oxidation and significant surface accumulation of DA and UA but repulsion of AA in neutral solutions. It was demonstrated that this sensor can separate AA, DA and UA oxidation into three well-defined DPV peaks at −0.004, 0.308 and 0.172 V (vs. SCE), respectively. Thus, the determination of DA and UA can be conducted in the presence of large amounts of AA. The sensor was highly sensitive with detection limit of 88 nM DA and 0.19 μM UA, which is superior to single DNA/GCE or Pp-ABSA/GCE. The advantage of this modified electrode was attributed to a co-operation of the 2-D fractal Pp-ABSA modified layer and the DNA cover layer. The mechanism was proposed as the p-electron stacking of the base pairs with the conjugated aromatic rings of the conductive dimer.

Acknowledgement

We gratefully acknowledge the financial support from National Natural Science Foundation of China (No. 20575062) and the Specialized Research Fund for the Doctoral Program of Higher Education (No. 20040358021).

References

[1] E.M. Boon, J.K. Barton, Charge transport in DNA, Curr. Opin. Struck. Biol. 12 (2002) 320–329.

[2] S. Delaney, J.K. Barton, Long-range DNA charge transport, J. Org. Chem. 68 (2003) 6475–6483.
[3] M.A. O'Neill, J.K. Barton, DNA charge transport: conformationally gated hopping through stacked domains, J. Am. Chem. Soc. 126 (2004) 11471–11483.
[4] M.A. O'Neill, J.K. Barton, DNA-mediated charge transport requires conformational motion of the DNA bases: elimination of charge transport in rigid glasses at 77 K, J. Am. Chem. Soc. 126 (2004) 13234–13235.
[5] S. Delaney, J.K. Barton, Charge transport in DNA duplex/quadruplex conjugates, Biochemistry 42 (2003) 14159–14165.
[6] T.T. Williams, D.T. Odom, J.K. Barton, Variations in DNA charge transport with nucleotide composition and sequence, J. Am. Chem. Soc. 122 (2000) 9048–9049.
[7] V.D. Lakhno, V.B. Sultanov, B.M. Pettitt, Combined hopping-superexchange model of a hole transfer in DNA, Chem. Phys. Lett. 400 (2004) 47–53.
[8] S. Laib, A. Krieg, DNA-intercalation on pyrene modified surface coatings, Chem. Commun. 44 (2005) 5566–5568.
[9] X.D. Su, Covalent DNA immobilization on polymer-shielded silver-coated quartz crystal microbalance using photobiotin-based UV irradiation, Biochem. Biophys. Res. Commun. 290 (2000) 962–966.
[10] S.J. Zeng, X.Q. Lin, Intercalation of epinephrine with calf-thymus ds-DNA, Chin. Chem. Lett. 12 (2001) 619–622.
[11] X.Q. Lin, L.P. Lu, X.H. Jiang, Voltammetric behaviour of dopamine at ct-DNA modified carbon fiber microelectrode, Microchem. Acta 143 (2003) 229–235.
[12] L.P. Lu, X.Q. Lin, Glassy carbon electrode modified with gold nanoparticles and DNA for the simultaneous determination of uric acid and norepinephrine under coexistence of ascorbic acid, Anal. Sci. 20 (2004) 527–530.
[13] X.H. Jiang, X.Q. Lin, Atomic force microscopy of DNA self-assembled on a highly oriented pyrolytic graphite electrode surface, Electrochem. Commun. 6 (2004) 873–879.
[14] X.Q. Lin, X.H. Jiang, L.P. Lu, DNA nano-netting intertexture on carbon electrodes, Chin. Chem. Lett. 5 (2004) 997–1000.
[15] X.Q. Lin, X.H. Jiang, L.P. Lu, DNA deposition on carbon electrodes under controlled DC potentials, Biosens. Bioelectron. 20 (2005) 1709–1717.
[16] J. Wang, M. Jiang, Toward genolelectronics: nucleic acid doped conducting polymers, Langmuir 16 (2000) 2269–2274.
[17] J.M. Gibbs, S.J. Park, D.R. Anderson, K.J. Watson, C.A. Mirkin, S.B.T. Nguyen, Polymer-DNA hybrids as electrochemical probes for the detection of DNA, J. Am. Chem. Soc. 127 (2005) 1170–1178.
[18] N. Lassalle, P. Mailley, E. Vieil, T. Livache, A. Roget, J.P. Correia, L.M. Abrantes, Electronically conductive polymer grafted with oligonucleotides as electrosensors of DNA preliminary study of real time monitoring by in situ techniques, J. Electroanal. Chem. 509 (2001) 48–57.
[19] J. Wang, M. Jiang, A. Fortes, B. Mukherjee, New label-free DNA recognition based on doping nucleic-acid probes within conducting polymer films, Anal. Chim. Acta 402 (1999) 7–12.
[20] M. Jiang, J. Wang, Recognition and detection of oligonucleotides in the presence of chromosomal DNA based on entrapment within conducting-polymer networks, J. Electroanal. Chem. 500 (2001) 584–589.
[21] S. Franceschi, O. Bordeau, C. Millerioux, E. Perez, P. Vicendo, I. Rico-Lattes, A. Moisand, Highly compacted DNA–polymer complexes obtained via new polynorbornene polycationic latexes with lactobionate counterion, Langmuir 18 (2002) 1743–1747.
[22] J. Cha, J.I. Han, Y. Choi, D.S. Yoon, K.W. Oh, G. Lim, DNA hybridization electrochemical sensor using conducting polymer, Biosens. Bioelectron. 18 (2003) 1241–1247.
[23] D.S. Minehan, K.A. Marx, S.K. Tripathy, Kinetics of DNA binding to electrically conducting polypyrrole films, Macromolecules (1994) 777–783.
[24] L.A. Thompson, J. Kowalik, M. Josowicz, J. Janata, Label-free DNA hybridization probe based on a conducting polymer, J. Am. Chem. Soc. 125 (2003) 324–325.
[25] R. Ceravolo, D. Volterrani, G. Gambaccini, et al., Presynaptic nigro-striatal function in a group of Alzheimer's disease patients with Parkinsonism: evidence from a dopamine transporter imaging study, J. Neural Transm. 111 (2004) 1065–1073.
[26] E.N. Liberopoulos, G.A. Miltiodous, M.S. Elisaf, Alcohol intake, serum uric acid concentrations, and risk of gout, Lancet 364 (2004) 246–247.
[27] C.R. Raj, T. Ohsaka, Electroanalysis of ascorbate and dopamine at a gold electrode modified with a positively charged self-assembled monolayer, J. Electroanal. Chem. 496 (2001) 44–49.
[28] H. Razmi, A. Azadbakht, Electrochemical characteristics of dopamine oxidation at palladium hexacyanoferrate film, electroless plated on aluminum electrode, Electrochim. Acta 50 (2005) 2193–2201.
[29] Y.F. Zhao, Y.Q. Gao, D.P. Zhan, et al., Selective detection of dopamine in the presence of ascorbic acid and uric acid by a carbon nanotubes-ionic liquid gel modified electrode, Talanta 66 (2005) 51–57.
[30] H.R. Zare, N. Nasirizadeh, M.M. Ardakani, Electrochemical properties of a tetrabromo-*p*-benzoquinone modified carbon paste electrode: application to the simultaneous determination of ascorbic acid, dopamine and uric acid, J. Electroanal. Chem. 577 (2005) 25–33.
[31] X.H. Jiang, X.Q. Lin, Immobilization of DNA on carbon fiber microelectrodes by using overoxidized polypyrrole template for selective detection of dopamine and epinephrine in the presence of high concentrations of ascorbic acid and uric acid, Analyst 130 (2005) 391–396.
[32] P. Ramesh, S. Sampath, Selective determination of uric acid in presence of ascorbic acid and dopamine at neutral pH using exfoliated graphite electrodes, Electroanalysis 16 (2004) 866–869.
[33] R. Aguilar, M.M. Davila, M.P. Elizalde, et al., Capability of a carbon-polyvinylchloride composite electrode for the detection of dopamine, ascorbic acid and uric acid, Electrochim. Acta 49 (2004) 851–859.
[34] T. Selvaraju, R. Ramaraj, Simultaneous determination of dopamine and serotonin in the presence of ascorbic acid and uric acid at poly(*o*-phenylenediamine) modified electrode, J. Appl. Electrochem. 33 (2003) 759–762.
[35] T. Liu, M.X. Li, Q.Y. Li, Electroanalysis of dopamine at a gold electrode modified with *N*-acetylcysteine self-assembled monolayer, Talanta 63 (2004) 1053–1059.
[36] Z.Q. Gao, H. Huang, Simultaneous determination of dopamine, uric acid and ascorbic acid at an ultrathin film modified gold electrode, Chem. Commun. 19 (1998) 2107–2108.
[37] S.Q. Wang, L.P. Lu, X.Q. Lin, A selective voltammetric method for uric acid detection at a glassy carbon electrode modified with electrodeposited film containing DNA and Pt–Fe(III) nanocomposites, Electroanalysis 16 (2004) 1734–1738.
[38] L. Fernandez, H. Carrero, Electrochemical evaluation of ferrocene carboxylic acids confined on surfactant clay modified glassy carbon electrodes: oxidation of ascorbic acid and uric acid, Electrochim. Acta 50 (2005) 1233–1240.
[39] L.F. Xiao, J. Chen, C.S. Cha, Elimination of the interference of ascorbic acid in the amperometric detection of biomolecules in body fluid samples and the simple detection of uric acid in human serum and urine by using the powder microelectrode technique, J. Electroanal. Chem. 495 (2000) 27–35.
[40] Q. Wang, D. Dong, N.Q. Li, Electrochemical response of dopamine at a penicillamine self-assembled gold electrode, Bioelectrochemistry 54 (2001) 169–175.
[41] F. Xu, M.G. Gao, L. Wang, G.Y. Shi, W. Zhang, L.T. Jin, J.Y. Jin, Sensitive determination of dopamine on poly(aminobenzoic acid) modified electrode and the application toward an experimental Parkinsonian animal model, Talanta 55 (2001) 329–336.
[42] I. Mav, M. Zigon, 1H NMR Study of the kinetics of substituted aniline polymerization. II. copolymerization of 2-methoxyaniline and 3-amino-benzenesulfonic acid, J. Polym. Sci., A, Polym. Chem. 39 (2001) 2482–2493.
[43] J.H. Fan, M.X. Wan, D.B. Zhu, Synthesis and characterization of water-soluble conducting copolymer poly(aniline-co-*o*-aminobenzenesulfonic acid), J. Polym. Sci., A, Polym. Chem. 36 (1998) 3013–3019.
[44] J.Y. Zhao, H. Wang, K.R. Cromack, A.J. Epstein, A.G. MacDiarmidl, Effect of sulfonic acid group on polyaniline backbone, J. Am. Chem. Soc. 113 (1991) 2665–2671.
[45] A. Lomander, W. Hwang, S. Zhang, Hierarchical self-assembly of a coiled-coil peptide into fractal structure, Nano Lett. 5 (2005) 1255.

[46] X.F. Li, Y. Wan, C.Q. Sun, Covalent modification of a glassy carbon surface by electrochemical oxidation of r-aminobenzene sulfonic acid in aqueous solution, J. Electroanal. Chem. 569 (2004) 79–87.
[47] M. Karabaliev, V. Kochev, Electrochemical investigations of cholesterol enriched glassy carbon supported lipid thin films, Biophys. Chemist. 103 (2003) 157–167.
[48] A.M. Oliveira-Brett, V.C. Diculescu, Electrochemical study of quercetin-DNA interactions: part I. Analysis in incubated solution, Bioelectrochemistry 64 (2004) 133–141.
[49] A.M. Oliveira-Brett, V.C. Diculescu, Electrochemical study of quercetin-DNA interactions part I. In situ sensing with DNA biosensors, Bioelectrochemistry 64 (2004) 143–150.
[50] J.A.P. Piedade, I.R. Fernandes, A.M. Oliveira-Brett, Electrochemical sensing of DNA–adriamycin interactions, Bioelectrochemistry 56 (2002) 81–83.